18-step Back-to-Back Voltage Source Converter with Pulse Interleaving Circuit for HVDC Application

Hye-Yeon Lee*, Jong-Kyou Jeong, Ji-Heon Lee**, Byung-Moon Han†, Nam-Sup Choi*** and Han-Ju Cha******

Abstract – This paper proposes an 18-step back-to-back (BTB) voltage source converter using four sets of 3-Level converter modules with auxiliary circuits to increase the number of steps. The proposed BTB voltage source converter has the independent control capability of active power and reactive power at the interconnected ac system. The operational feasibility of the proposed BTB converter was verified through many simulations with PSCAD/EMTDC software. The feasibility of hardware implementation was verified through experimental results with a scaled hardware prototype. The proposed BTB converter could be widely applied for interconnecting the renewable energy source to the power grid.

Keywords: multi-step converter, BTB (Back-To-Back) converter, pulse interleaving circuit, HVDC (High Voltage DC transmission system)

1. Introduction

Recently, due to energy exhaustion and environmental protection, electric power generation using renewable energy sources has come into wide use all over the world. As the capacity of generated power increases, it is interconnected with utility grids using a BTB voltage source converter.

Voltage source converters are divided into two types based on switching pattern. A PWM converter has one bridge with many switching operations within one power cycle. A multi-step converter has two or more bridges with one switching operation within one power cycle.

The switching loss of a PWM converter is very high because there are many switching operations within one power cycle. The high switching loss makes it difficult for high power applications. The multi-step converter has low switching loss because there is only one switching operation within one power cycle. However, the multi-converter should have a large number of bridges and coupling transformers for overlapping the output voltage waveform.

Various methods have already been developed to increase the number of steps in the output voltage waveform of the multi-step converter [1], [2]. The simplest method is to increase the number of bridges and the number of coupling transformers. However, this method has a weak point of large size and high cost due to the increased number of bridges and transformers.

A method to insert auxiliary transformers between the main transformer and the bridge was proposed to complement the weak point, instead of increasing the number of main transformers [3]. However, this method also has a weak point that the auxiliary transformer is very difficult to build because of its complicated connection structure.

In order to solve the weak point of the above method, a method to insert an auxiliary circuit in the DC link side was proposed by several researchers [4]. The auxiliary circuit, which consists of a mid-tap transformer and a full-bridge inverter, generates a three-level step that is superposed to the DC capacitor voltage to reduce the harmonic level of the output voltage. However, the mid-tap transformer for superposing the output waveform has a bigger size and lower performance due to the inaccuracy of the mid tap point.

The authors already proposed a 36-step BTB converter which consists of a 3-level half-bridge inverter and a normal transformer, replacing the full-bridge inverter and the mid-tap transformer [5]. However, the 36-step BTB converter requires four units of the main transformer and two units of auxiliary transformers at the sending end and the receiving end, respectively.

This paper proposes an 18-step BTB voltage source converter using four sets of 3-level converter modules with auxiliary circuits to increase the number of steps. The proposed BTB voltage source converter has an independent control capability of active power and reactive power at the interconnected ac system.

2. Back-to-Back Operation

The BTB converter can be utilized to interconnect two

† Corresponding Author: Department of Electrical Engineering Myongji University, Yongin, Korea. (erichan@mju.ac.kr)
* HVDC Research Team, LS Industrial Systems, Anyang, Korea. (hleea@lsis.biz)
** Department of Electrical Engineering Myongji University, Yongin, Korea. (jjuk486@mju.ac.kr)
*** Division of Electrical Electronic Communication and Computer Engineering, Chonnam National University, Yeosu, Korea. (nschoi@chonnam.ac.kr)
****Department of Electrical Engineering, Chungnam National University. (hjcha@cnu.ac.kr).
Received: January 13, 2010; Accepted: March 9, 2010

AC power systems with the same or a different power frequency. A large-scale wind power farm can be interconnected with the AC power grid with the BTB power converter. The BTB converter consists of two voltage source converters, which share the DC capacitors as shown in Fig. 1. Depending on the active power flow from one AC system to another, one voltage source converter works as a rectifier, while another works as an inverter. The BTB converter has to control the power flow from one AC system to another, and regulates the reactive power at both AC systems to regulate the bus voltage [6], [7]. So, each converter has to have two degrees of control freedom.

The BTB converter operated in PWM mode can control active and reactive power independently by adjusting the modulation index and firing angle. However, the BTB converter operated in multi-step mode cannot control the active and reactive power independently because the modulation index is fixed. So, a special scheme is required to endow two degrees of control freedom.

The allocation of a control function for each converter is dependenting on the direction of power flow. When the power is transmitted from the system A to B, the converter A performs the constant DC voltage control and the reactive power control, while the converter B performs the active and reactive power control. When the power is transmitted from the system B to A, the opposite control function is selected.

Fig. 2(a) shows a generalized voltage source converter connected to the AC source through a reactor, which represents an equivalent circuit for the rectifier or inverter part interconnected with the AC source, neglecting the resistance of the coupling reactor. The phasor relationship for the converter voltage, the source voltage and the converter current is described in Fig. 2(b).

According to the phasor diagram, the following equations can be derived with the geometric relationship.

$$V_C \sin\delta = I_C X_C \cos\theta \tag{1}$$

$$V_C \cos\delta - V_S = I_C X_C \sin\theta \tag{2}$$

The active and reactive powers can be derived as the following two equations.

$$P = V_S I_S \cos\theta = \frac{V_C V_S}{X_C} \sin\delta \tag{3}$$

$$Q = V_S I_S \sin\theta = \frac{-(V_S{}^2 - V_S V_C \cos\delta)}{X_C} \tag{4}$$

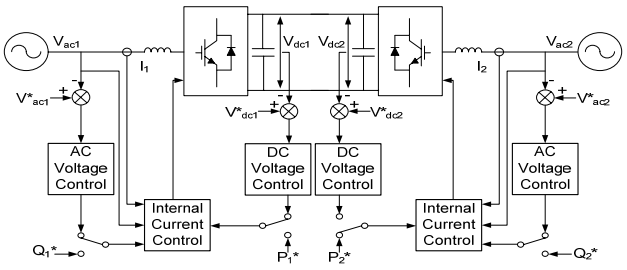

Fig. 1. BTB converter for AC system interconnection.

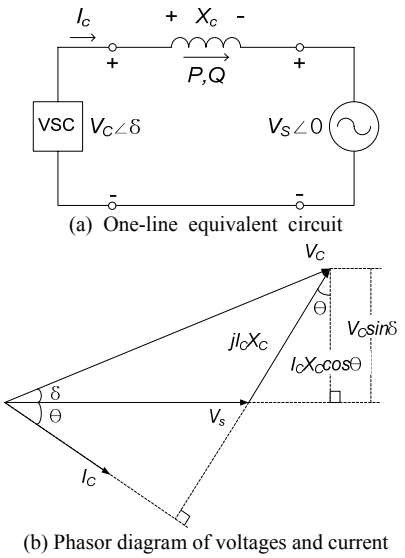

Fig. 2. Active and reactive power calculation.

Considering the 3-phase system, the active and reactive powers can be represented as the following equations.

$$P = \frac{3V_C V_S}{X_C} \sin\delta \tag{5}$$

$$Q = \frac{-3(V_S{}^2 - V_C V_S \cos\delta)}{X_C} \tag{6}$$

Combining (5) and (6) above and using the root formula of second order equations, two equations for the V_C and δ with respect to P and Q can be derived.

$$V_C = \sqrt{\frac{P^2 X_C^2 + \left(3V_S^2 - QX_C\right)^2}{9V_S^2}} \tag{7}$$

$$\delta = \sin^{-1}\left(\frac{PX_C}{3V_S V_C}\right) \tag{8}$$

Using Equations (7) and (8), the magnitude and phase angle of converter output voltage can be functionally determined by the given active and reactive powers.

3. 18-Step Voltage Source Converter

Fig. 3 shows a basic configuration of an 18-step converter with a pulse interleaving circuit, which was introduced in [8], [9]. This converter consists of a main transformer and a 3-level voltage source converter with an auxiliary circuit composed of a 3-level half-bridge and a single-phase transformer.

The voltages across the upper part and lower part of a 3-level converter are the sum of the DC capacitor voltage $v_{dc}/2$ and the injected voltage through the transformer v_{aux} as described in Equations (9) and (10).

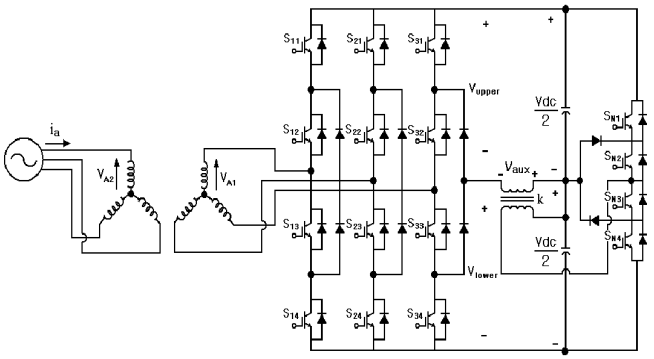

Fig. 3. 18-step converter using auxiliary circuit.

$$V_{upper} = v_{dc}/2 + v_{aux} \quad (9)$$
$$V_{lower} = v_{dc}/2 - v_{aux} \quad (10)$$

The AC output voltage of the converter can be regulated by controlling the injected voltage v_{aux}, which is determined by the switching pattern and the turn ratio of the injection transformer. So, the injected voltage V_{aux} has three values of 0, $kV_{dc}/2$, $-kV_{dc}/2$. Since the auxiliary 3-level half-bridge operates in a periodic manner at every 120°, it generates a pulse train with a frequency 3 times 60Hz. The turn ratio of transformer k should be determined to minimize the harmonic level of the output voltage.

Fig. 4 shows the output voltage waveform at each part of the proposed 18-step converter. Fig. 4(a) shows the output voltage waveform of an auxiliary circuit. It has three pulses within one cycle of power frequency, which means that one pulse is generated every 120° of power frequency. Figs. 4(b) and 4(c) show the voltage waveform across the upper part and the lower part of a 3-level converter. The voltage value is the sum or difference between the DC voltage $v_{dc}/2$ and the injected voltage v_{aux}. Figs. 4(d) and 4(e) show the line-to-line voltage and the phase voltage at the output terminal.

The turn ratio of auxiliary transformer should be optimized because the magnitude of injected voltage affects the harmonic level of the output voltage.

The Fourier series analysis for the waveform shown in Fig. 4(e) can be represented by Eq (11).

$$v_{AN} = \sum_{n=1}^{\infty} \frac{2V_{dc}}{n\pi}[k\cos\frac{n\beta_0}{2} + (1-k)\cos n(\frac{\beta_0}{2} + \beta_1)]\sin n\omega t \quad (11)$$

Where, the magnitude of each harmonic component can be represented by Eq. (12).

$$V_{AN,n} = \frac{2V_{dc}}{n\pi}[k\cos\frac{n\beta_0}{2} + (1-k)\cos n(\frac{\beta_0}{2} + \beta_1)] \quad (12)$$

The 5th harmonic is a major component that affects the output waveform of the inverter. So, n was substituted by 5 in Eq. (12), and the values of β_0 and β_1 were set by 20° respectively. The value of k was determined by 0.574 to make Eq. (12) equal to zero.

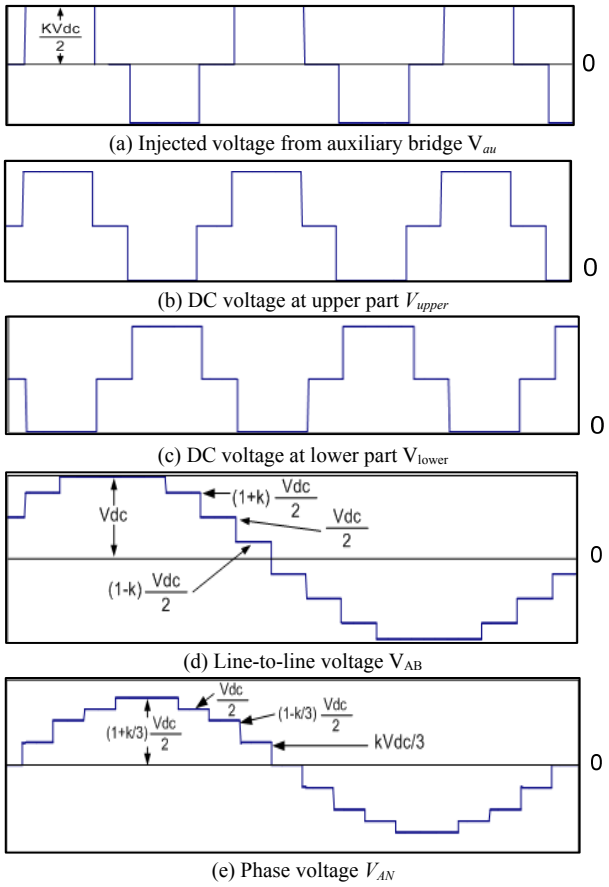

Fig. 4. Waveforms of 18-step converter.

4. Proposed 18-Step BTB Converter

This paper proposes a BTB converter that is composed of four sets of an 18-step converter module as shown in Fig. 5. The AC side of the rectifier or inverter part is connected in series, while the DC side is connected in shunt. The proposed BTB converter controls the active and reactive power independently by adjusting the firing angle of upper module α_1 and the firing angle of lower module α_2 differently.

Fig. 6(a) shows a single-phase equivalent circuit for the rectifier or inverter part of the proposed BTB converter which is interconnected with the AC power system. Fig. 6(b) shows a phasor diagram for the output voltage of each

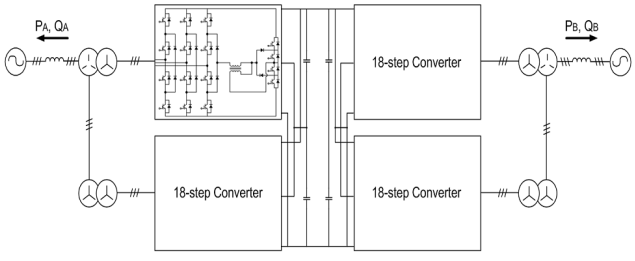

Fig. 5. Configuration of 18-step BTB HVDC system.

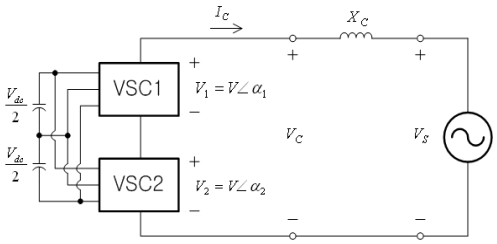

(a) One-line equivalent circuit

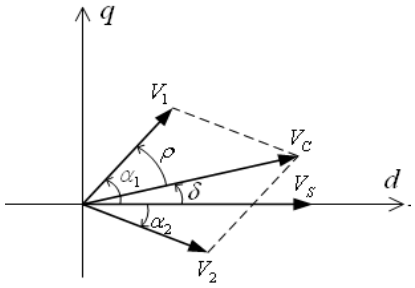

(b) Phasor diagram of converter voltage

Fig. 6. Operation principle of proposed BTB converter.

module, the resultant output voltage of the converter, and the source voltage, when the upper and lower module operates with a different firing angle.

The magnitude and angle of converter output voltage V_C with respect to the source voltage V_S can be mathematically determined by the value of α_1 and α_2.

The principle to determine the upper and lower firing angle, α_1 and α_2 with respect to the source voltage V_S can be derived using the phasor diagram.

If the angle between V_C and V_1, or V_C and V_2 is defined as ρ, the following two relationships are obtained.

$$V_C = 2V\cos\rho \tag{13}$$

$$\rho = \alpha_1 - \delta = \delta - \alpha_2 \tag{14}$$

The relationship of δ with respect to α_1 and α_2, and the relationship of V_C with respect to α_1 and α_2 can be expressed as the following two equations, assuming that the maximum voltage of V_C is equal to 1.15 time V_S.

$$\delta = \frac{\alpha_1 + \alpha_2}{2} \tag{15}$$

$$V_C = 1.15V_S\cos\left(\frac{\alpha_1 - \alpha_2}{2}\right) \tag{16}$$

The upper and lower firing angle α_1 and α_2 can be expressed as the following equations, combining (17) and (18) above.

$$\alpha_1 = \delta + \cos^{-1}\left(\frac{V_C}{1.15V_S}\right) \tag{17}$$

$$\alpha_2 = \delta - \cos^{-1}\left(\frac{V_C}{1.15V_S}\right) \tag{18}$$

Therefore, the value of α_1 and α_2 can be determined for the given P and Q, inserting the value of V_C and δ obtained from (7) and (8) into (17) and (18).

5. Simulation

The operational feasibility of the proposed BTB converter for an HVDC system was verified using computer simulation with PSCAD/EMTDC software. The power circuit is modeled using circuit elements, switches, and transformers, while the controller is modeled using built-in control modules. The circuit parameter used in the simulation is shown in Table 1.

Fig. 7 shows the controller structure for the proposed BTB converter, in which only one part at converter A is shown because converter B has an identical structure. The proposed BTB converter can control the active and reactive powers at each part of the power system by controlling the firing angle control for each converter module as explained in the previous section.

When converter A transmits real power to converter B, the measured value of DC voltage v_{dc} follows the reference value v_{dc}*. The reference value of active current I_{dA}* is obtained from the measured value of active current I_{dB} in converter B. The measured value of reactive current I_{qA} and active current I_{dB} follow reference value I_{qA}* and I_{dB}* through the current control algorithm. The AC current controller has the same configuration as used in normal

Table 1. Simulation circuit parameter

Bus Voltage	3φ, 220 [V]
Frequency	60 [Hz]
Source Inductance	2 [mH]
DC Capacitor	3000 [uF]
Main Transformer	110:110
Auxiliary Transformer	110:63
System Power Rating	10 [kVA]

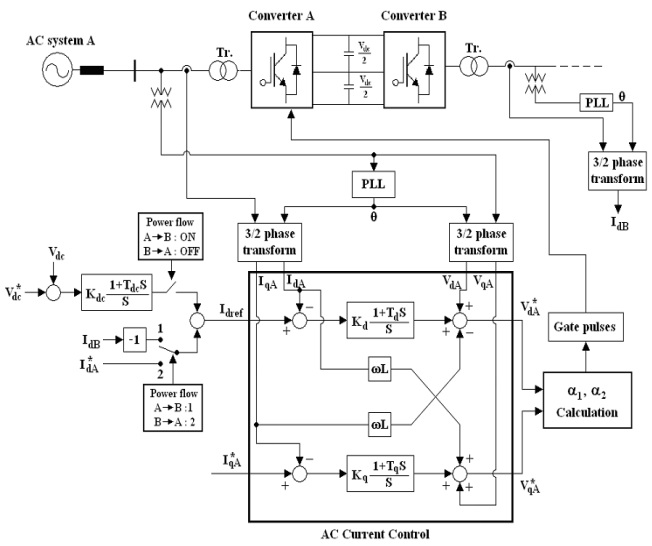

Fig. 7. Converter controller at system A-side.

controller for converter. The reference values of d-q transformed AC system voltage v_{dA}* and v_{qA}* are used to determine the value of V_C and δ. The values of α_1 and α_2 are obtained from V_C and δ using the relationship described in Equations (17) and (18).

Table 2 shows the simulation scenario that was used in the operation analysis of the proposed BTB converter. The controller starts operation after 0.5s when the simulation starts. It is assumed that the direction of the power flow is from system A to B between 0.5s and 2.0s, and it is suddenly changed from system B to A at 2.0s. In order to analyze the control performance of active and reactive power, the reference values of active and reactive power are changed according to each operation mode from M1 to M5.

Fig. 8 shows the simulation results obtained to confirm the whole system operation. Since the control structure of system A is exactly the same as that of system B, all control parameters have the same values as the opposite sign. Figs. 8(a) and 8(b) show the variations of converter power angle δ, upper firing-angle α_1, and lower firing-angle α_2. The values of α_1 and α_2 are corresponding to those shown in Fig. 6 and the values of δ are corresponding to those in Table 1.

Table 2. Simulation scenario

Mode	M1	M2	M3	M4	M5
Time[s]	0.5~1.0	1.0~2.0	2.0~3.0	3.0~4.0	4.0~5.0
V_{dc}*[V]	350				
i_{dA}*[A]	V_{dc} control			-15	-25
i_{qA}*[A]	0	20	0	15	-30
i_{dB}*[A]	0	10	25	V_{dc} control	
i_{qB}*[A]	0	30	-15	0	15
P_A[KW]	0	2.2	5.5	-3.3	-5.5
Q_A[Kvar]	0	4.4	0	3.3	-6.6
P_B[KW]	0	-2.2	-5.5	3.3	5.5
Q_B[Kvar]	0	6.6	-3.3	0	3.3

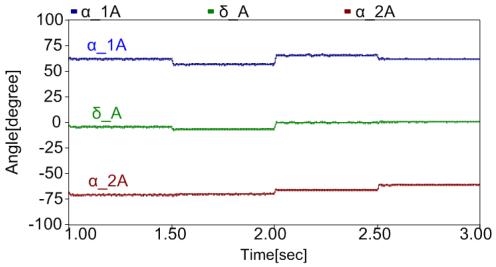

(a) Converter power angle δ_A, upper firing-angle α_{1A}, and lower firing-angle α_{2A} at converter A

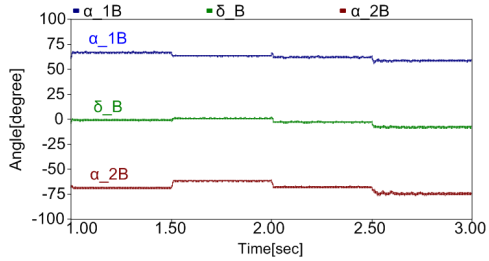

(b) Converter power angle δ_B, upper firing-angle α_{1B}, and lower firing-angle α_{2B} at converter B

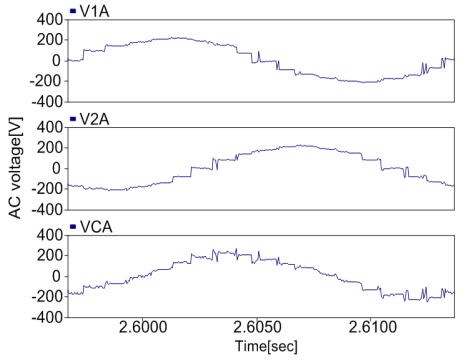

(c) Superposed voltage V_{CA}, and V_{1A}, V_{2A} at converter A

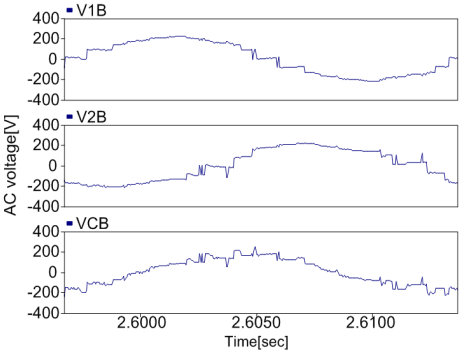

(d) Superposed voltage V_{CB}, and V_{1B}, V_{2B} at converter B

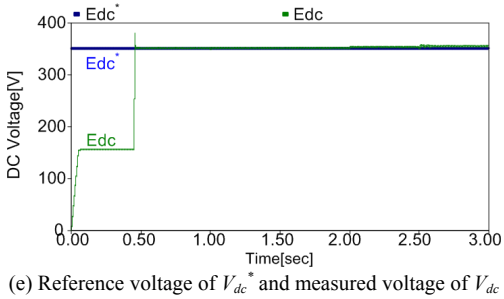

(e) Reference voltage of V_{dc}* and measured voltage of V_{dc}

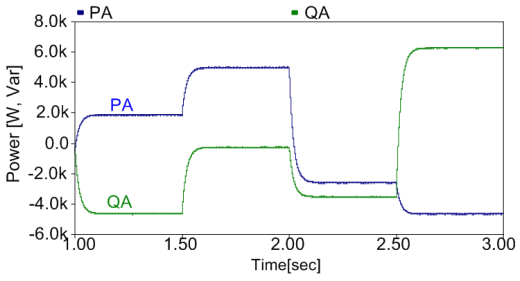

(f) Transmitted active power P_A and reactive power Q_A at converter A

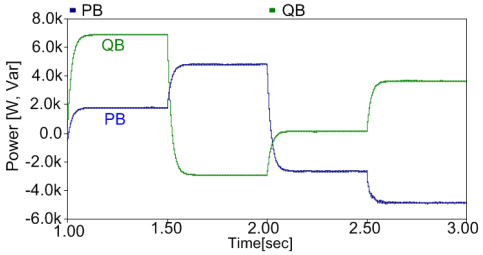

(g) Transmitted active power P_B and reactive power Q_B at converter B

Fig. 8. Simulation results of proposed BTB HVDC system.

Figs. 8(c) and 8(d) show the variations of each converter output voltage and superposed output voltage. Fig. 8(e) shows the control performance of DC link voltage. The DC link voltage is initially charged with 350V for the convenience of simulation, so that the BTB converter could start to operate at 0.5s. The measured value of DC link voltage tracks the reference value of 350V without severe transients.

Fig. 8(f) shows the variation of active and reactive powers transmitted from AC system A to converter A, which confirms the active and reactive powers to system A can be controlled independently. Fig. 8(g) shows the variation of active and reactive powers transmitted from converter B to AC system B. The active power has the same value as in Fig. 8(f), while the reactive power has a different value. This confirms that the BTB converter has independent control capability for the active and reactive powers at both terminals.

6. Hardware Experiment

A scaled model for the proposed BTB converter was built and tested to confirm the feasibility of hardware implementation as shown in Fig. 9. The hardware system consists of a source simulator and two 18-step converters. The experimental parameters of the scaled model were shown in Table 3.

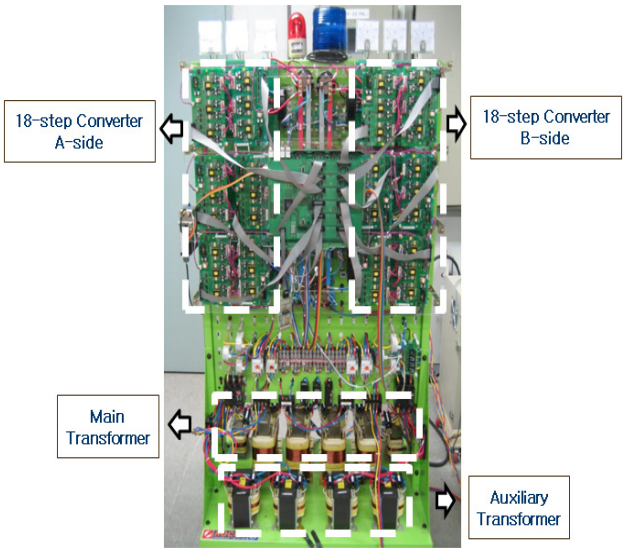

Fig. 9. Scaled model of BTB converter.

Table 3. Hardware experiment parameters

Bus Voltage	3φ, 220 [V]
Frequency	60 [Hz]
Source Inductance	2 [mH]
DC Capacitor	330 [uF]
Main Transformer	110:110
Auxiliary Transformer	110:63
System Power Rating	2 [kVA]

The control board is composed of a main board and an extension board. The main processor is a 32-bit floating-point DSP (TMS320vc33, Texas Instruments). PWM pulse generation was implemented by EPLD (EP1K50QC208, ALTERA). The same EPLD was used in the extension board to implement PWM pulse generation.

The experimental scenario of the scaled model was shown in Table 4, in which 10 operational modes were considered to confirm the independent control of active and reactive power.

Fig. 10 shows the experimental results when the active and reactive power changes according to the scenario. Fig. 10(a) shows the active and reactive power of each side converter. This confirms that the BTB converter has independent control capability for active and reactive powers at both terminals. Fig. 10(b) shows the DC-link voltage of each side converter. The DC-link voltage control is carried out by each side converter depending on the flow direction of the active power. The measured DC voltage tracks the reference value without a large amount of transient. Fig. 10(c) shows the power angle variation in which the angular relationship of $\alpha_1 - \delta = \delta - \alpha_2$ was shown in the vector diagram. Fig 10(d) shows the output voltage of the upper and lower converter, the total output voltage, and the injected voltage through the auxiliary transformer. It is verified that the upper voltage and the lower voltage are summed up to make a total output voltage. The auxiliary transformer injects a voltage waveform with a frequency three times the power frequency.

Table 4. Experimental scenario

Mode	M1	M2	M3	M4	M5
V_{dcA}^*, V_{dcB}^*[V]	200				
I_{dA}^*[A]	DC Voltage Control				
I_{qA}^*[A]	0	0	-2.273	2.273	0
I_{dB}^*[A]	0	1.136	2.273	3.409	0
I_{qB}^*[A]	0	-2.273	2.273	0	0
Mode	M6	M7	M8	M9	M10
I_{dA}^*[A]	1.136	2.273	3.409	0	0
I_{qA}^*[A]	-2.273	2.273	0	0	0
I_{dB}^*[A]	DC Voltage Control				
I_{qB}^*[A]	0	0	-2.273	2.273	0

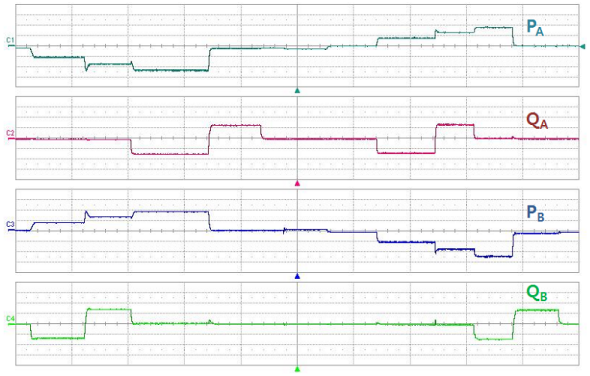

(a) Active power P_A, P_B and reactive power Q_A, Q_B at each end

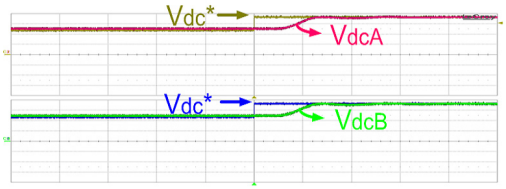

(b) Reference voltage of V_{dc}^{*} and DC-link voltage of each converter

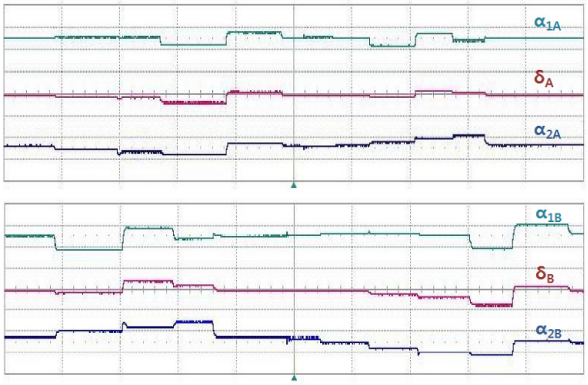

(C) Converter power angle δ_A, δ_B, upper firing-angle α_{1A}, α_{2A}, and lower firing-angle α_{1B}, α_{2B}

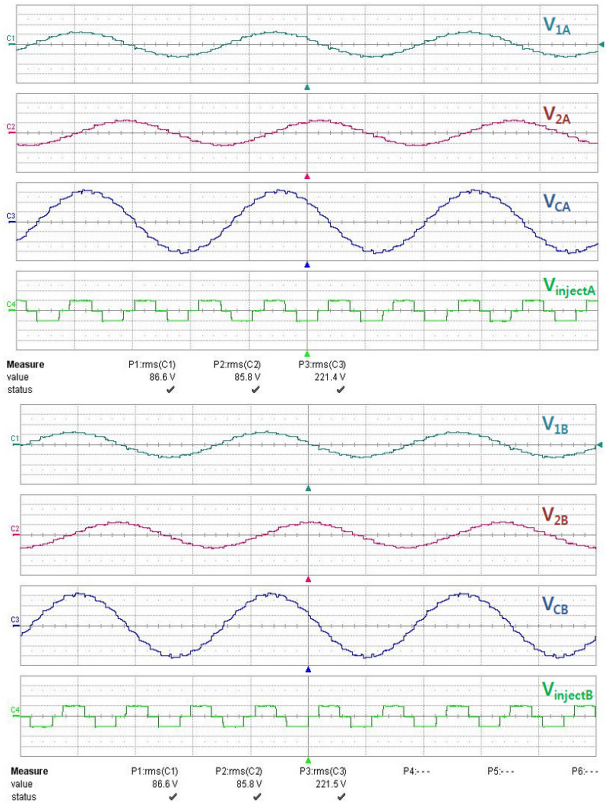

(d) Output voltage at upper and lower converter, Total output voltage, Injected voltage from auxiliary transformer

Fig. 10. Experimental results of scaled model.

7. Conclusion

This paper proposes an 18-step BTB voltage source converter using four sets of 3-Level converter modules with auxiliary circuits to increase the number of steps.

The proposed BTB voltage source converter has an independent control capability of active power and reactive power at the interconnected ac system. The operational feasibility of the proposed system was verified through computer simulations with PSCAD/EMTDC software.

The feasibility of hardware implementation was verified through experimental results with a scaled hardware model. The proposed converter would have a smaller size and lower cost than the previously developed system and can be widely applied for interconnecting two AC power systems with a different power frequency and a large-scale wind power farm with an AC power system.

Acknowledgements

This work was supported by the 2010 research fund of Myongji University in Korea, and the research fund of MKE through the Research Center for Intelligent Microgrid in Myongji University.

References

[1] S. Mori, et al., "Development of large static var generator using self-commutated inverters for improving power system stability", *IEEE Trans. on Power System*, vol. 8, no. 1, pp. 371-377, Feb. 1993.

[2] C. Schauder, et. al., "Development for a ±100MVar static condenser for voltage control of transmission systems", *IEEE Trans. on Power Delivery*, vol. 10, no. 3, pp. 1486-1493, July 1995.

[3] D. Ramey, "*Design, Installation, and Operation of American Electric Power (AEP) 320MVA Unified Power Flow Controller (UPFC)*", EPRI (Electric Power Research Institute), Palo Altos, CA, Tech. Rep. TR-113839, Nov. 1999.

[4] S. Masukawa and S. Iida, "A Method for Reducing Harmonics in Output Voltages of a Double-Connected Inverter", *IEEE Trans. on Power Electronics*, vol. 9, no. 5, pp. 543-550, Sept. 1994.

[5] B. Han, S. Baek, B. Bae, J. Choi, "Back-to-Back HVDC system using a 36-step voltage source converter", *IEE Proc. Gener. Transm. Distrib.,* vol. 153, no. 6, pp. 677-683, Nov. 2006.

[6] L. Yonghe, J. Arrillaga and N. Watson, "EMTDC Assessment of a New Type of VSC for Back to back HVdc Interconnections", *International Conference on Power system Transients-IPST 2003 in New Orleans*, USA, pp. 1-5.

[7] L. Yonghe, J. Arrillaga and N. Watson, "Multi-level voltage sourced conversion by voltage reinjection at six times the fundamental frequency", *IEE Proc. on Electrical Power Application*, vol. 149, no. 3, pp. 201-207, May 2002.

[8] K. Oguchi, et. al., "A Novel Six-Phase Inverter Sys-

tem with 60-Step Output Voltage for High-Power Motor Drives", *IEEE Trans. on Industry Applications*, vol. 35, no.5, pp. 1141-1149, July 1995.

[9] K. Oguchi, Y. Maki and Y. Sunaga, "Three-Phase Multilevel Voltage Source Converters with Low Switching Frequencies and Less-Distorted Input Voltages," *Industry Applications Society Annual Meeting*, Conference Record of the 1993, IEEE, vol. 2, pp. 870-878, Oct. 1993.

Hye-Yeon Lee received her B.S. and M.S. in Electrical Engineering from Myongji University, Korea, in 2008 and 2010, respectively. Currently she is a research engineer with the HVDC Research Team at LS Industrial Systems, Korea. Her research interests are in power electronics applications for FACTS and HVDC systems.

Jong-Kyou Jeong received his B. S. and Master degrees in Electrical Engineering from Myongji University, Korea, in 2008 and 2010 respectively. He is currently a Ph. D. candidate at Myongji University. His research interests are in power electronics applications for custom power and distributed generation.

Ji-Heon Lee received his B. S. and Master degrees in Electrical Engineering from Myongji University, Korea, in 2008 and 2010 respectively. He is currently a Ph. D. candidate at Myongji University. His research interests are in power electronics applications for custom power and distributed generation.

Byung-Moon Han (S'91-M'92-SM'00) received his B.S. in Electrical Engineering from Seoul National University, Korea, in 1976, and his M.S. and Ph.D. from Arizona State University in 1988 and 1992, respectively. He was with the Westinghouse Electric Corporation as a Senior Research Engineer in the Science and Technology Center. Currently, he is a Professor in the Department of Electrical Engineering at Myongji University, Korea. His research interests are in power electronics applications for FACTS, custom power, and distributed generation.

Nam-Sup Choi received his B.S. degree in Electrical Engineering from Korea University in 1987. He received his M.S. degree and D.S. degree in Electrical Engineering at the Korean Advanced Institute of Science and Technology (KAIST), South Korea, in 1989 and 1994, respectively. He is currently a professor in the Division of Electrical Electronic Communication and Computer Engineering, Chonnam National University, South Korea. His research interests include Modeling and the control of power converters and systems.

Hanju Cha received the B.S degree in electrical engineering form Seoul National University, Seoul, Korea, the M.S degree from Pohang Institude of Science and Technology, Korea, and the Ph.D. degree from Texas A&M University, College station, in 1988, 1990 and 2004, respectively, all in electrical engineering. From 1990 to 2001, he was with LG industrial system, Anyang, Korea, where he was engaged in the development of power electronics and adjustable speed drives.

In 2005, he joined the Department of Electrical Engineering, Chungnam National University, Daejeon, Korea. His current research interests are high-power converter, ac/dc, dc/ac and ac/ac converter topologies, power quality, and utility interface issues for distributed energy system and microgrids.